

Radial Viscous Fingers and Diffusion-Limited Aggregation: Fractal Dimension and Growth Sites

G rard Daccord and Johann Nittmann

Etudes et Fabrication Dowell Schlumberger, 42003 St. Etienne, France

and

H. Eugene Stanley

Center for Polymer Studies and Department of Physics, Boston University, Boston, Massachusetts 02215

(Received 16 October 1985)

We show that fractal viscous fingers can be formed in a Hele-Shaw cell with radial symmetry, thereby permitting their study—for the first time—without the complicating effects of boundary conditions such as those present in the conventional linear cell. We find—for a wide range of shear-thinning fluids, flow rates, and plate separations—that radial viscous fingers have a fractal dimension $d_f = 1.70 \pm 0.05$, the same as diffusion-limited aggregation. We also quantitatively measure the set of growth sites and compare with diffusion-limited aggregation.

PACS numbers: 47.90.+a

Recently, there has occurred an explosive burst of activity focused on the wide range of physical phenomena that occur when a low-viscosity liquid is forced into a high-viscosity liquid.¹⁻¹¹ Particularly striking is the fact that under certain conditions the resulting viscous fingers are fractal objects.² This means that the fractal dimension d_f can be used as a new *quantitative* parameter that can be used to characterize an important liquid instability.

The utility of the above remarks is compromised by the fact that experiments are typically carried out in a rectangular Hele-Shaw cell, and the apparent value of d_f is a strong function of the width of the cell [cf. Fig. 6 of Ref. 2]. As a result, it is difficult to interpret experimental findings on d_f , and the entire utility of being able to characterize the viscous-fingering instability by a quantitative parameter is called into question. Moreover, the question of what boundary conditions to use for the lateral walls of the Hele-Shaw cell is quite subtle. To interpret viscous-finger patterns in terms of a statistical mechanical model, one assumes that particles launched from one end of the cell are *absorbed* if they strike the lateral walls.

The purpose of this Letter is to describe a Hele-Shaw cell that differs fundamentally from the conventional Hele-Shaw cell: It has radial symmetry and overcomes all the above objections. Accordingly, it becomes possible to attempt—for the first time—a meaningful comparison between experimental results and model simulations.

Our radial cell¹¹ consists of a pair of circular glass plates which are 1 m in diameter and 2 cm thick [Fig. 1(a)]. The plates are held apart by spacers so that their separation is a *constant* distance b (typically $b = 0.5$ mm). The high-viscosity fluid occupies all the space between the plates until suddenly water is forced through a circular inlet in the center of the cell. After

some care with spacing and other experimental conditions, we were able to generate viscous fingers with a striking radial geometry [cf. Fig. 1(b)]. Our viscous-fingering phenomena appear to be quite universal, being independent, e.g., of the microscopic structure of the liquids.¹² To demonstrate this, we made experiments with several high-viscosity polymer solutions and also latex (an aqueous suspension of polymer spheres).¹³ In all cases the viscosity ratio was roughly 10^2 – 10^4 , depending on the velocity of the low-viscosity water.

The quantitative analysis of a radial viscous finger (RVF) is carried out by several independent methods; all begin with machine digitization of the finger, replacing the cell with a lattice of $N = 2^{16}$ points. We calculated d_f using several methods:

(i) Sandbox method¹⁴: About every lattice point in the finger, one forms an imaginary $L \times L$ square box. The number $N(L)$ of finger points is counted and averaged over all possible lattice points as center. A log-log plot of $N(L)$ vs L has slope d_f [Fig. 1(c)].

(ii) Radius of gyration (R_g) method¹⁴: Here several photographs of the finger are taken at successive stages of growth. For each photograph, R_g is measured. A log-log plot against finger mass has slope $1/d_f$.

(iii) Density-density correlation function method¹⁴: Here one randomly chooses a cluster point and calculates the probability that cluster points a distance r away are connected to it. The slope of a log-log plot against r is the codimension, $d_f - d$.

The estimates of d_f obtained by the three methods are consistent with one another, and we conclude that

$$d_f(\text{radial cell}) = 1.70 \pm 0.05, \quad (1)$$

which is considerably larger than the values for even the widest Hele-Shaw cell studied experimentally.²

What microscopic phenomena give rise to this fractal geometry? To answer this question, we devised an experimental procedure to measure quantitatively the growth of a finger. We subtracted two successive photographs of the finger taken at 1-sec intervals (Fig. 2). We found that the finger grows only by consecutive splitting of the leading tips: essentially no growth oc-

curs in the "screened" interior regions. This differs from dendritic growth, which often shows stable tips but proliferating side branches.¹⁵ Our experimental results are also in quantitative agreement with simulations of diffusion-limited aggregation¹⁶ (DLA); e.g., our density correlation function falls off with distance with an exponent of -1.3 ± 0.1 , while the DLA value is¹⁴ -1.1 .

Interpretation.—Because of the *qualitative* visual similarity between our data [Fig. 1(b)] and a DLA cluster, it is tempting to conclude that DLA accurately describes viscous fingering in a radial geometry. This conclusion is supported by the *quantitative* similarity of the respective values of d_f for DLA and RVF. On careful comparison between the experimental photographs of RVF and off-lattice simulations of DLA,¹⁴ we do note a few qualitative differences: (i) The "spokes" of the RVF are straight, relative to the "sinuous" spokes of DLA.¹⁴ (ii) There is more "foliage" growing on the DLA spokes compared to the relatively barren impression of the RVF spokes.¹⁴ (iii) If one makes a histogram of tip splitting angle, measured

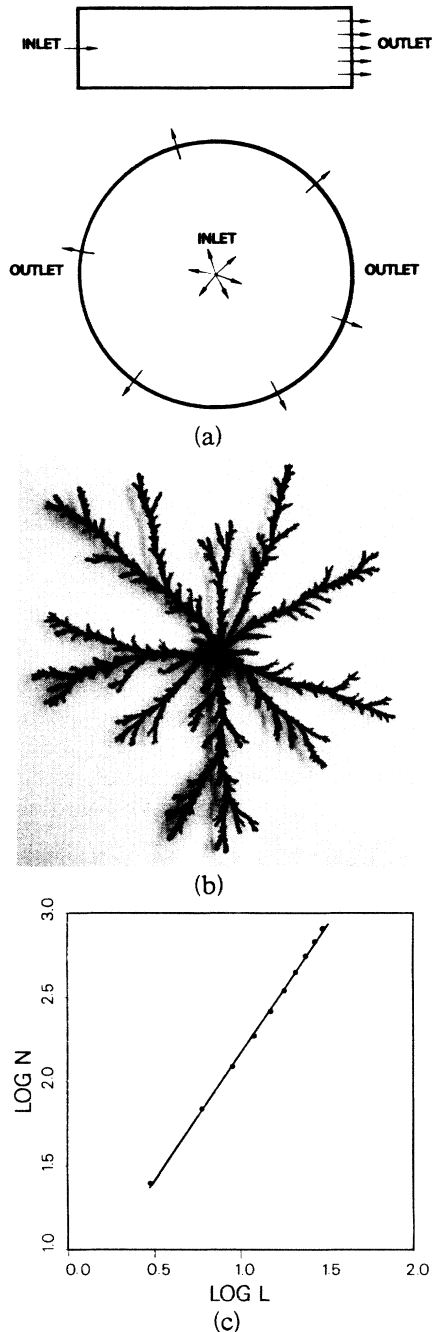


FIG. 1. (a) Schematic illustration of the lateral and radial cells, (b) typical radial viscous finger, and (c) analysis of the fractal dimension by method (i).

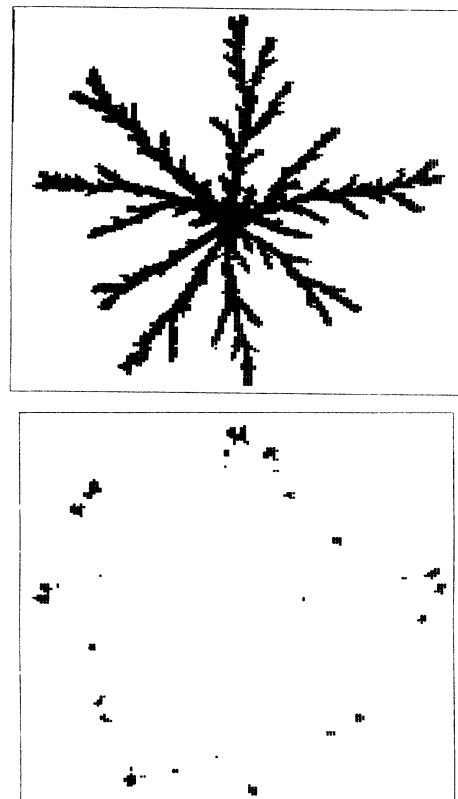


FIG. 2. The "growth region" of a typical radial viscous finger, obtained by subtracting the images of the same finger photographed at slightly different times. The fact that the growth regions are only on the tips is a striking proof of the high degree of screening.

at each of the finger bifurcations, one finds that the RVF distribution is narrower than for DLA.¹⁷

Although there may be some qualitative differences in visual appearance between RVF and DLA, there are striking mathematical similarities—at least for the case of Newtonian fluids. In DLA the local probability field $\phi(r,t)$ satisfies the Laplace equation $\text{div grad}\phi = 0$, with the boundary conditions that $\phi = 0$ at the aggregate and $\phi = 1$ at the launch of the random walkers. Growth is proportional to the gradient of $\phi(r,t)$; this is similar to the flow velocity u for Newtonian fluids in a Hele-Shaw cell, which is proportional to the gradient of the pressure, $P(r)$. We assume that the low-viscosity fluid has negligible viscosity and has constant pressure $P(r)$ independent of distance r from the center. With the incompressibility condition $\text{div}u = 0$ we then obtain a Laplace equation for the pressure distribution in the high-viscosity fluid.

For shear-thinning fluids, however, the growth rate or flow velocity is

$$u \propto (\text{grad}P)^m, \tag{2}$$

where $m = 1/n'$ and $n' - 1$ is the slope of a log-log plot of viscosity versus shear rate.¹⁸ Depending on the type of fluid used, we found n' to vary between 0.4 and 0.1. Applying the constraint $\text{div}u = 0$, we find that the pressure has to follow¹⁹

$$\text{div}(|\text{grad}P|^{m-1}\text{grad}P) = 0. \tag{3}$$

The solution of Eq. (3) is

$$P(r) = [R^{(m-1)/m} - r^{(m-1)/m}] / [R^{(m-1)/m} - 1] \tag{4a}$$

for $m \neq 1$,

$$P(r) = 1 - \log r / \log R \text{ for } m = 1, \tag{4b}$$

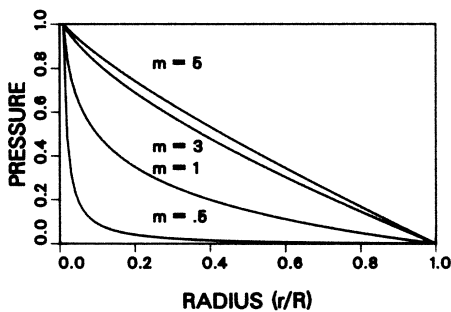


FIG. 3. Dependence of the pressure field $P(r)$ on the distance r from the center of a radial Hele-Shaw cell. Shown are several curves for different values of the parameter $m = 1/n'$, where n' is the shear-thinning exponent. The Newtonian fluids analyzed previously concern the case $m = 1$. We used high-viscosity fluids with n' in the range 0.1–0.4 so that $m > 1$.

with the boundary condition $P = 1$ at $r = 1$ and $P = 0$ when $r = R$ (see Fig. 3). The case $m = 1$ corresponds to DLA (or dielectric breakdown¹⁹ or gradient-governed growth²⁰). Combining (2) and (4), we see that non-Newtonian fluids will follow the same growth law $u \sim 1/r$. Because of the $(\text{grad}P)^m$ term in (2), non-Newtonian growth for $m > 1$ shows more tendency to grow on the tip than in the bulk compared with Newtonian growth. However, this tendency is balanced by the much flatter overall pressure distribution of Eq. (4a) [see Fig. 3], which makes the differences between the local pressure gradients at tip and bulk smaller compared with Newtonian growth. That non-Newtonian effects will not change the growth rate (to first approximation) explains the close proximity in fractal dimension between DLA and RVF.²²

In summary, we have tested the degree to which viscous fingers may be modeled by DLA. To this end, we have introduced a new radial cell which avoids the problems in interpretation that arise from the lateral walls of a traditional Hele-Shaw cell. We find that the radial fingers thus generated have a well-defined and reproducible fractal dimension, with a value close to that predicted for off-lattice DLA; indeed, we found quantitative agreement with DLA for all the fractal properties we measured. The practical choice of the fluids used guaranteed essentially zero interfacial tension, a high viscosity ratio, and almost “plug flow” displacement of the polymer solution by the water. All three properties appear to be important for obtaining fractal growth.²³ Linear stability analysis by Chuoke, Van Meurs, and Van der Poel²⁴ predicts that for immiscible fluids, the finger thickness λ_m (the “characteristic wavelength of growth”) scales linearly with the plate separation. For miscible fluids, Paterson²³ also put forward a linear scaling relation based on a viscous

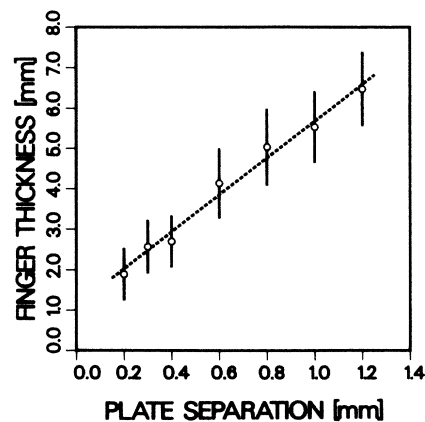


FIG. 4. Dependence of the finger width λ_m (the “characteristic wavelength”) upon the separation b of the Hele-Shaw plates for the non-Newtonian fluid scleroglucan (shear-thinning exponent $n' = 0.15$).

dissipation theory. It differs from early work in that λ_m does not depend on the viscosity difference and flow rate. We measured λ_m as a function of b , with b varying from 0.2 to 1.2 mm (almost an order of magnitude). We find (Fig. 4) a linear growth law. The slope is roughly ~ 4.6 , close to the value proposed by Paterson; however, it is not clear that Paterson's theory can be applied to our fluids since the dissipation mechanisms are considerably different in our non-Newtonian fluids.

We wish to thank M. Bourlion for technical assistance in several stages of the experiments, T. A. Witten and J. D. Sherwood for helpful discussions, and F. Rondelez for helpful comments on the manuscript.

- ¹L. Paterson, Phys. Rev. Lett. **52**, 1621 (1984).
²J. Nittmann, G. Daccord, and H. E. Stanley, Nature (London) **314**, 141 (1985).
³J. Maher, Phys. Rev. Lett. **54**, 1498 (1985); T. Maxworthy, to be published.
⁴C. Tang, Phys. Rev. A **31**, 1977 (1985); D. Bensimon, to be published.
⁵E. Ben Jacob, R. Godbey, N. D. Goldenfeld, J. Koplik, H. Levine, T. Mueller, and L. M. Sander, Phys. Rev. Lett. **55**, 1315 (1985).
⁶L. P. Kadanoff, J. Stat. Phys. **39**, 267 (1985); S. Liang, to be published.
⁷R. Lenormand and C. Zarcone, Phys. Rev. Lett. **54**, 2226 (1985).
⁸Closely related are the problems associated with solidification. See T. Vicsek, Phys. Rev. Lett. **53**, 2281 (1984); J. Szép, J. Certi, and J. Kertész, J. Phys. A **18**, L413 (1985).
⁹A. J. DeGregoria and L. W. Schwartz, to be published.
¹⁰G. Tryggvason and H. Aref, to be published; D. A. Kessler and H. Levine, to be published.
¹¹Radial cells were also considered in L. Paterson, J. Fluid Mech. **113**, 513 (1981).
¹²Thus far, we have found fractal viscous fingers only when using two liquids with very small interfacial tension. Although many liquids of practical concern are miscible, some are not. The addition of surface tension introduces a length scale, above which we might expect that the fingers will also be fractal. This expectation is based on the presence of tip splitting *even for nonmiscible liquids* (see, e.g., Fig. 7 of Ref. 2). Recent studies of tip-splitting phenomena suggest that as soon as tip splitting occurs, fractal phenomena set in [J. Nittmann and H. E. Stanley, to be published]. Experimental work designed to test this possibility is under way.
¹³Shear-thinning fluids represent a wide class of industrial fluids: most of the polymer solutions and many common suspensions (cements, latexes, clay suspensions, etc). Our latex spheres can be replaced by the particulate matter form-

ing a clay, with no substantial change in results [see the recent work of H. Van Damme, F. Obrecht, P. Levitz, and L. Gatineau, Nature (to be published).] If our findings generalize from latex spheres to clay, it is natural to assume that they may generalize to realistic random porous media—a possibility supported by recent experiments on model porous materials [J.-D. Chen and D. Wilkinson, Phys. Rev. Lett. **55**, 1892 (1985); K. J. Måløy, J. Feder, and T. Jøsang, Phys. Rev. Lett. **55**, 2688 (1985)].

¹⁴See, e.g., the recent review by P. Meakin, in *On Growth and Form: Fractal and Non-Fractal Patterns in Physics*, edited by H. E. Stanley and N. Ostrowsky (Nijhoff, Dordrecht, 1985), p. 69. Although the “spokes” of DLA seem sinuous compared to our experimental patterns, the fractal dimension d_{\min} of the minimum path connecting two points is unity for *both* problems: see, e.g., P. Meakin, I. Majid, S. Havlin, and H. E. Stanley, J. Phys. A **17**, L975 (1984).

¹⁵H. Honjo, S. Ohta, and Y. Sawada, Phys. Rev. Lett. **55**, 841 (1985). See also the recent work by Y. Sawada, A. Dougherty, and J. P. Gollub, to be published.

¹⁶T. A. Witten and L. M. Sander, Phys. Rev. Lett. **47**, 1400 (1981).

¹⁷In fact, if one measures the angle between the main trunk and the side branches, one finds a remarkably narrow distribution centered about 40° .

¹⁸R. B. Bird, R. C. Armstrong, and D. Haffager, *Dynamics of Polymeric Liquids* (Wiley, New York, 1977), Vol. 1.

¹⁹Note that our non-Newtonian growth model is different from the dielectric breakdown model [L. Niemeyer, L. Pietronero, and H. Wiesmann, Phys. Rev. Lett. **52**, 1033 (1984)], which follows the growth law Eq. (2) but with a pressure distribution $P(r)$ following the Laplace equation. For $m=1$, the two models are identical but for $m \neq 1$, quite different structures are obtained.

²⁰J. D. Sherwood and J. Nittmann, J. Phys. (Paris) (to be published).

²¹An analogous argument can be developed for $m < 1$.

²²A note about our viscosity ratio: The underlying equations describing DLA are similar to the equations describing viscous fingering of fluids with infinite viscosity ratio in a Hele-Shaw cell. Our experimental system has a *finite* viscosity ratio. However, the fact that the viscosity of our polymer solution increases rapidly with decreasing shear rate will delay even further the slowly moving interface in the deep invaginations of the RVF. This makes our system seem even closer to the ideal limiting case of infinite viscosity ratio (which is equivalent to constant potential on the cluster, as in DLA).

²³L. Paterson, Phys. Fluids **28**, 26 (1985), has recently performed experiments with miscible Newtonian fluids for which only a partial displacement normal to the glass plates is observed. His structures were ramified but not as developed as in the non-Newtonian case.

²⁴R. L. Chuoke, P. Van Meurs, and C. J. Van der Poel, J. Pet. Technol. **11**, 64 (1959).

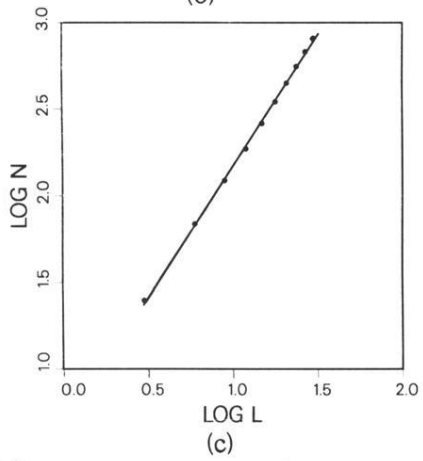
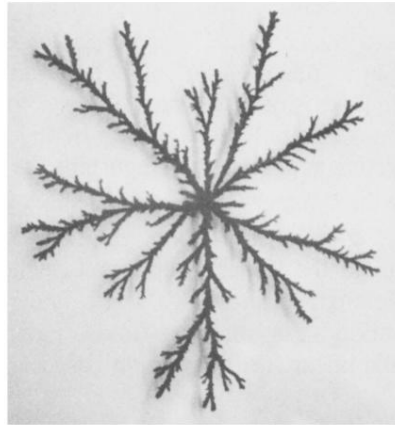
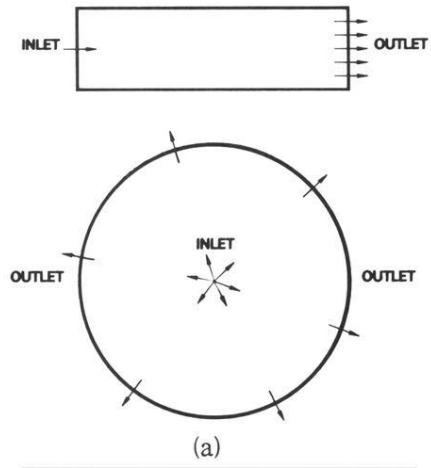


FIG. 1. (a) Schematic illustration of the lateral and radial cells, (b) typical radial viscous finger, and (c) analysis of the fractal dimension by method (i).

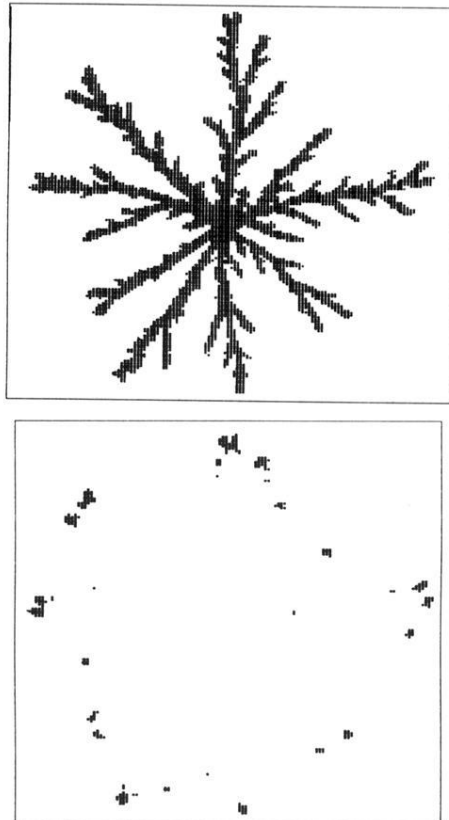


FIG. 2. The “growth region” of a typical radial viscous finger, obtained by subtracting the images of the same finger photographed at slightly different times. The fact that the growth regions are only on the tips is a striking proof of the high degree of screening.